

Non-Centrosymmetric Ammonium Rare Earth Nitrates $(\text{NH}_4)_2\text{Ln}(\text{NO}_3)_5 \cdot 4\text{H}_2\text{O}$ – Crystal Structure, Crystal Growth and Optical Properties

Ladislav Bohatý,^[a] Roland Fröhlich,^[b] Peter Held,^[a] and Petra Becker*^[a]

Keywords: Crystal growth / Refractive indices / SHG phase matching / Structure elucidation / Rare earths

For crystals of $(\text{NH}_4)_2\text{Ln}(\text{NO}_3)_5 \cdot 4\text{H}_2\text{O}$ ($\text{Ln} = \text{La}, \text{Ce}, \text{Pr}, \text{Nd}$), the piezoelectric and the pyroelectric effect was demonstrated unambiguously. X-ray structure determination shows that all four compounds are isomorphic, with monoclinic, non-centrosymmetric space group Cc , and are further isomorphic to the related rubidium compounds $\text{Rb}_2\text{Ln}(\text{NO}_3)_5 \cdot 4\text{H}_2\text{O}$. Large single crystals of the colourless compounds $(\text{NH}_4)_2\text{La}(\text{NO}_3)_5 \cdot 4\text{H}_2\text{O}$ and $(\text{NH}_4)_2\text{Ce}(\text{NO}_3)_5 \cdot 4\text{H}_2\text{O}$ were

grown. On the basis of determined precise refractive indices and their dispersion in the wavelength region 0.365–1.083 μm , phase-matching conditions for collinear second harmonic generation were analyzed. In both crystals, type I phase matching can be realized for wavelengths from 0.893 μm (La) or 0.892 μm (Ce) to the near IR, where first absorption bands appear.

Introduction

In 1885, Auer v. Welsbach succeeded in separating “didymium” into praseodymium and neodymium by using fractional crystallization of the corresponding monoclinic ammonium rare earth nitrate tetrahydrates, $(\text{NH}_4)_2\text{Pr}(\text{NO}_3)_5 \cdot 4\text{H}_2\text{O}$ and $(\text{NH}_4)_2\text{Nd}(\text{NO}_3)_5 \cdot 4\text{H}_2\text{O}$, from nitric acid.^[1] Crystals of ammonium didymium nitrate tetrahydrate had been synthesized and identified already several years before,^[2] together with the related lanthanum and cerium compounds;^[3] their monoclinic symmetry had been described first on the basis of morphological measuring.^[4–6] In all following investigations, the crystals were treated with (centrosymmetric) monoclinic prismatic symmetry, as was suggested by the crystal morphology. Also from arguments of crystal morphology, the isomorphism of $(\text{NH}_4)_2\text{Ln}(\text{NO}_3)_5 \cdot 4\text{H}_2\text{O}$ and the related rubidium compounds $\text{Rb}_2\text{Ln}(\text{NO}_3)_5 \cdot 4\text{H}_2\text{O}$ ($\text{Ln} = \text{La}, \text{Ce}, \text{Pr}, \text{Nd}$)^[7] as well as thallium compounds^[8] was concluded.

In later X-ray structure determinations, $\text{Rb}_2\text{Ln}(\text{NO}_3)_5 \cdot 4\text{H}_2\text{O}$ ($\text{Ln} = \text{La}, \text{Ce}, \text{Pr}, \text{Nd}$) were described with (non-centrosymmetric) space group symmetry Cc ,^[9–11] while for $(\text{NH}_4)_2\text{Ln}(\text{NO}_3)_5 \cdot 4\text{H}_2\text{O}$, the symmetry $C2/c$ was given^[12–14]. Here, the question arises whether the isomorphism of the rubidium and the ammonium compounds, suggested by the crystal morphology, could even be a “true” structural isomorphism (demanding identical space group symmetry). This is of particular interest, since in the group of alkali metal rare earth nitrates, the potassium compounds

$\text{K}_2\text{Ln}(\text{NO}_3)_5 \cdot 2\text{H}_2\text{O}$ ($\text{Ln} = \text{La}, \text{Ce}$), which crystallize with non-centrosymmetric space group symmetry $Fdd2$,^[15,16] possess remarkable nonlinear optical properties,^[17–19] and our recent analysis of the optical properties of the rubidium rare earth nitrate tetrahydrates, $\text{Rb}_2\text{Ln}(\text{NO}_3)_5 \cdot 4\text{H}_2\text{O}$, proves the attractiveness of these crystals for optical frequency conversion as well.^[11] Motivated by this, crystals of $(\text{NH}_4)_2\text{La}(\text{NO}_3)_5 \cdot 4\text{H}_2\text{O}$ and $(\text{NH}_4)_2\text{Ce}(\text{NO}_3)_5 \cdot 4\text{H}_2\text{O}$ were tested in our laboratories by crystal physical methods for non-centrosymmetry. The test revealed unambiguously the occurrence of the piezoelectric and the pyroelectric effect, thus giving definite proof for non-centrosymmetry of the crystals. Encouraged by these results, a redetermination of the crystal structures of $(\text{NH}_4)_2\text{Ln}(\text{NO}_3)_5 \cdot 4\text{H}_2\text{O}$ ($\text{Ln} = \text{La}, \text{Ce}, \text{Pr}, \text{Nd}$), the growth of large single crystals of the colourless La and Ce compounds, which served as the basis for crystal physical investigations, and determination of linear optical properties were carried out.

Results and Discussion

Crystal Growth

From our growth experiments, large single crystals of dimensions up to $2.5 \times 2.5 \times 3$ cm and a mass of 25–35 g for both $(\text{NH}_4)_2\text{La}(\text{NO}_3)_5 \cdot 4\text{H}_2\text{O}$ and $(\text{NH}_4)_2\text{Ce}(\text{NO}_3)_5 \cdot 4\text{H}_2\text{O}$ were obtained (for an example, see Figure 1). The usual disturbances that occur in the region of the initial seed crystal can clearly be seen in Figure 1. In the progress of crystal growth, however, they vanished, and flawless crystals of optical quality, which allow the measurement of high-precision refractive indices, resulted. The morphology of the crystals appears similar to that of crystals of $\text{Rb}_2\text{Ln}(\text{NO}_3)_5 \cdot 4\text{H}_2\text{O}$ ($\text{Ln} = \text{La}, \text{Ce}$); however, in general only fewer forms

[a] Institut für Kristallographie, Universität zu Köln, Zùlpicher Str. 49b, 50674 Köln, Germany
Fax: +49-221-470-4963
E-mail: petra.becker@uni-koeln.de

[b] Organisch-Chemisches Institut, Universität Münster, Corrensstr. 40, 48149 Münster, Germany

occur. As in the case of the rubidium compounds, for the ammonium compounds the morphology is dominated by the pedions (001) and (00 $\bar{1}$) and domes {110} and { $\bar{1}\bar{1}0$ }. Additionally, the domes { $\bar{1}\bar{1}1$ }, {11 $\bar{1}$ } and the pedions (100) and ($\bar{1}00$) are present in all crystals. Minor faces are (10 $\bar{1}$), (101), {11 $\bar{2}$ }, { $\bar{1}\bar{1}2$ } and {111} (Figure 1). The well-developed faces of the crystals were used as reference for the preparation of oriented samples. Crystal physical properties reported in this work are related to a Cartesian system $\{\vec{e}_i\}$ that is defined with respect to the crystallographic system $\{\vec{a}_i\}$ as follows: $\vec{e}_2 \parallel \vec{a}_2$, $\vec{e}_3 \parallel \vec{a}_3$, $\vec{e}_1 = \vec{e}_2 \times \vec{e}_3$. For our setting, the longitudinal piezoelectric effect d'_{111} for directions of the face normals $\vec{h}(100)$ and $\vec{h}(001)$ is positive.

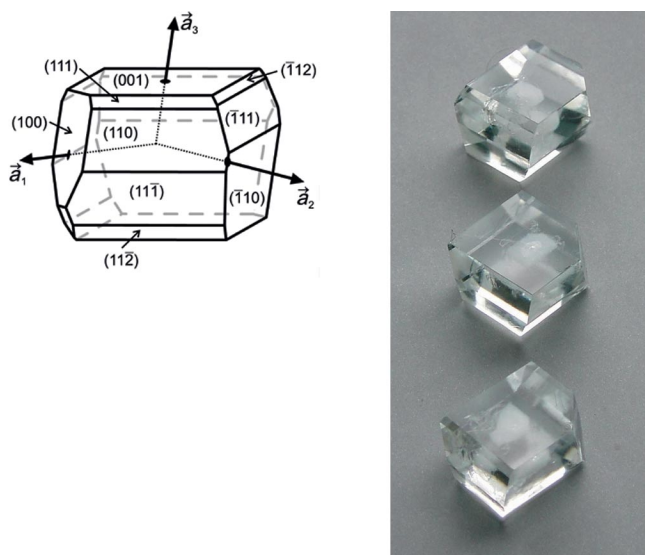


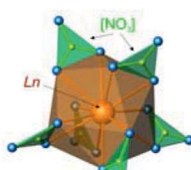
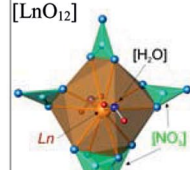
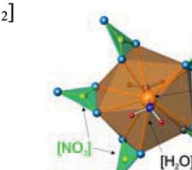
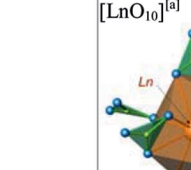

Figure 1. Left: typical morphology of grown crystals of $(\text{NH}_4)_2\text{-Ln}(\text{NO}_3)_5 \cdot 4\text{H}_2\text{O}$ ($\text{Ln} = \text{La}, \text{Ce}$); face indices and crystallographic axes $\{\vec{a}_i\}$ are indicated. Right: examples of grown crystals of $(\text{NH}_4)_2\text{-Ce}(\text{NO}_3)_5 \cdot 4\text{H}_2\text{O}$ with dimensions of ca. $2.5 \times 2.5 \times 3$ cm. In each crystal the cloudy region of the seed crystal can clearly be distinguished from the undisturbed crystal parts of optical grade.

Crystal Structure

Rare earth nitrate hydrates of general composition $\text{A}_2\text{Ln}(\text{NO}_3)_5 \cdot n\text{H}_2\text{O}$ ($\text{A} = \text{monovalent cation}$, $n \neq 0$) are structurally known so far for the large lanthanides ($\text{La}, \text{Ce}, \text{Pr}, \text{Nd}$) only. They belong to four different families that are characterized by space group symmetry and the particular coordination surroundings of the rare earth cation. For the centrosymmetric monohydrates (with $\text{A} = \text{Na}, \text{Ag}$) structural units $[\text{Ln}(\text{NO}_3)_6]$ with $[\text{NO}_3]$ groups as bidentate ligands are found, while for the dihydrates and tetrahydrates, structural units $[\text{Ln}(\text{NO}_3)_5(\text{H}_2\text{O})_2]$ are present. For the two non-centrosymmetric families (Table 1), all $[\text{NO}_3]$ groups act as bidentate ligands. Only for the centrosymmetric ($C2/c$) dihydrates are monodentate $[\text{NO}_3]$ ligands found, resulting in a tenfold coordination of the lanthanides. An overview with references is given in Table 1.

The results of our piezoelectric and pyroelectric measurements on large single crystals of $(\text{NH}_4)_2\text{La}(\text{NO}_3)_5 \cdot 4\text{H}_2\text{O}$ and $(\text{NH}_4)_2\text{Ce}(\text{NO}_3)_5 \cdot 4\text{H}_2\text{O}$ show the occurrence of a longitudinal piezoelectric effect (reported also 60 years ago^[29] for crystals of the cerium compound) as well as the pyroelectric effect for directions perpendicular to the a_2 axis. This indisputably restricts the possible monoclinic symmetry to point group m instead of $2/m$, that was used in all earlier structure determinations. Our crystal structure analysis reveals that all four investigated ammonium rare earth nitrate tetrahydrates $(\text{NH}_4)_2\text{Ln}(\text{NO}_3)_5 \cdot 4\text{H}_2\text{O}$ with $\text{Ln} = \text{La}, \text{Ce}, \text{Pr}$ and Nd are isomorphous, with monoclinic non-centrosymmetric space group symmetry Cc and lattice parameters as summarized in Table 3. Furthermore, they are isomorphic to the related rubidium compounds $\text{Rb}_2\text{Ln}(\text{NO}_3)_5 \cdot 4\text{H}_2\text{O}$ with $\text{Ln} = \text{La}, \text{Ce}, \text{Pr}, \text{Nd}$.^[11] As for the rubidium compounds, the prominent structural unit of ammonium rare earth nitrate tetrahydrates is a distorted icosahedral coordination polyhedron $[\text{LnO}_{12}]$ of the rare earth atoms, in which ten oxygen ligands belong to five nitrate groups coordinating in a bidentate fashion and the remaining two oxygen ligands are oxygen atoms of water

Table 1. Structurally known rare earth nitrate hydrates with general composition $\text{A}_2\text{Ln}(\text{NO}_3)_5 \cdot n\text{H}_2\text{O}$ ($n \neq 0$).

	$\text{Na}_2\text{Ln}(\text{NO}_3)_5 \cdot \text{H}_2\text{O}$	$\text{Ag}_2\text{Ln}(\text{NO}_3)_5 \cdot \text{H}_2\text{O}$	$\text{K}_2\text{Ln}(\text{NO}_3)_5 \cdot 2\text{H}_2\text{O}$	$\text{Rb}_2\text{Ln}(\text{NO}_3)_5 \cdot 4\text{H}_2\text{O}$	$(\text{NH}_4)_2\text{Ln}(\text{NO}_3)_5 \cdot 4\text{H}_2\text{O}$	$\text{Cs}_2\text{Ln}(\text{NO}_3)_5 \cdot 2\text{H}_2\text{O}$
$\text{Ln} =$	Ce, Pr, Nd	Ce	La, Ce, Pr, Nd	La, Ce, Pr, Nd	La, Ce, Pr, Nd	La, Ce, Nd
space group	$P2_1/c$	$P2_1/c$	$Fdd2$	Cc	Cc	$C2/c$
Ln coordination surrounding	$[\text{LnO}_{12}]$	$[\text{LnO}_{12}]$	$[\text{LnO}_{12}]$	$[\text{LnO}_{12}]$	$[\text{LnO}_{12}]$	$[\text{LnO}_{10}]^{[a]}$
						
References	Ce ^[20] , Pr ^[21] , Nd ^[22]	Ce ^[23]	La–Nd ^[16] , La ^[15] , Ce ^[17] , Pr ^[24] , Nd ^[25]	La–Nd ^[11] , La, Ce ^[9] , Ce ^[10]	this work	La ^[26] , Ce ^[27] , Nd ^[28]

[a] For $\text{Ln} = \text{Ce}, \text{Nd}$, only. For $\text{Ln} = \text{La}$ the coordination surrounding is similar to that in rubidium and ammonium rare earth nitrate tetrahydrates.

molecules, leading to the structural building block $[\text{Ln}(\text{NO}_3)_5(\text{H}_2\text{O})_2]^{2-}$ (Figure 2 and Table 1), as it was already found in earlier structure determinations of the ammonium compounds.^[12–14] The $[\text{Ln}(\text{NO}_3)_5(\text{H}_2\text{O})_2]$ groups are arranged in layers parallel to (001) that alternate with layers of $[\text{NH}_4]^+$ cations and H_2O along the a_3 axis (Figure 2). The resulting sheetlike structure corresponds to a distinct cleavage of the crystals parallel to (001). Within each layer of $[\text{NH}_4]^+$ and H_2O , the ammonium groups and the water molecules are separated, being arranged in two sublayers parallel to (001), one with ammonium groups and one with water molecules only, which are stacked along the a_3 axis (Figure 2). In analogy to the coordination surroundings of rubidium atoms in $\text{Rb}_2\text{Ln}(\text{NO}_3)_5 \cdot 4\text{H}_2\text{O}$, the two symmetrically inequivalent $[\text{NH}_4]^+$ groups in $(\text{NH}_4)_2\text{Ln}(\text{NO}_3)_5 \cdot 4\text{H}_2\text{O}$ are surrounded either by ten oxygen atoms, three of them belonging to H_2O and the remaining seven belonging to six $[\text{NO}_3]$ groups [second coordination sphere of N(6)], or by seven oxygen atoms, two of which belong to H_2O and five to four $[\text{NO}_3]$ groups [second coordination sphere of N(7)]. All attempts of structure refinements with other conceivable mutual arrangements of H_2O molecules and $[\text{NH}_4]^+$ groups yielded unreasonably short distances of hydrogen positions, thus supporting the isomorphism of crystals of $(\text{NH}_4)_2\text{Ln}(\text{NO}_3)_5 \cdot 4\text{H}_2\text{O}$ to $\text{Rb}_2\text{Ln}(\text{NO}_3)_5 \cdot 4\text{H}_2\text{O}$ as stated above. It should still be noted that in the case of $(\text{NH}_4)_2\text{Nd}(\text{NO}_3)_5 \cdot 4\text{H}_2\text{O}$ the refinement of the structure with inverted atom position parameters yielded a slightly lower R value (by 0.001), while the interatomic distances and bond angles did not undergo any significant changes. Here, a further detailed investigation is necessary. Note that the crystal structure of $(\text{NH}_4)_2\text{Ln}(\text{NO}_3)_5 \cdot 4\text{H}_2\text{O}$ sets an example for a case in which usual

structure checking computer routines are misleading and additional information from other investigations, for example, from measurement of crystal physical properties, is needed. In analogy with the Ln positions of the structure of $\text{Rb}_2\text{Ln}(\text{NO}_3)_5 \cdot 4\text{H}_2\text{O}$, the heavy lanthanide atoms in $(\text{NH}_4)_2\text{Ln}(\text{NO}_3)_5 \cdot 4\text{H}_2\text{O}$ occupy pseudo-centrosymmetric positions. While acentricity is clearly indicated by the refinement results (particularly by the Flack parameter) for the former compounds because of the strong scattering contribution of Rb (which occupies a non-centrosymmetric position), this can not be expected for the latter because of the very low f'' values of the anomalous scattering of nitrogen and oxygen [located on non-centrosymmetric positions in the case of $(\text{NH}_4)_2\text{Ln}(\text{NO}_3)_5 \cdot 4\text{H}_2\text{O}$] by using Mo radiation.

Optical Properties

Refractive index data were measured at 11 discrete wavelengths and were corrected for the refractive index of air (see Experimental Section). All data given here correspond to the corrected values. A modified Sellmeier equation of the type

$$n^2(\lambda) = D_1 + \frac{D_2}{(\lambda^2 - D_3)} - D_4\lambda^2$$

was fitted to the measured refractive index data. In Figure 3, the principal refractive indices and their dispersion, together with the Sellmeier functions are illustrated, and the

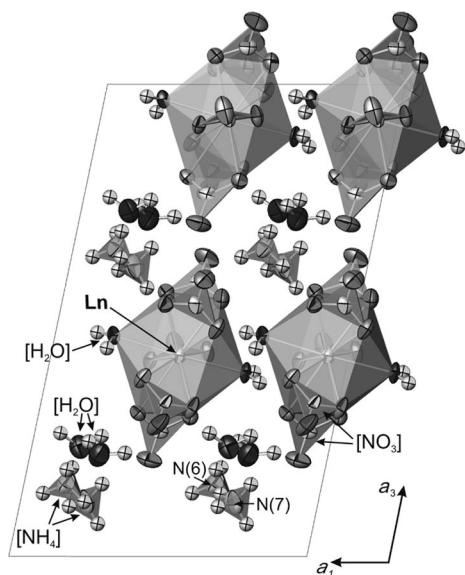


Figure 2. View along $-\vec{a}_2$ of a section of the crystal structure of the isomorphic compounds $(\text{NH}_4)_2\text{Ln}(\text{NO}_3)_5 \cdot 4\text{H}_2\text{O}$ (Ln = La, Ce, Pr, Nd) using the Ce compound as example. Non-hydrogen atoms are shown as 50% probability displacement ellipsoids and hydrogen atoms as spheres with arbitrary radius for clarity.

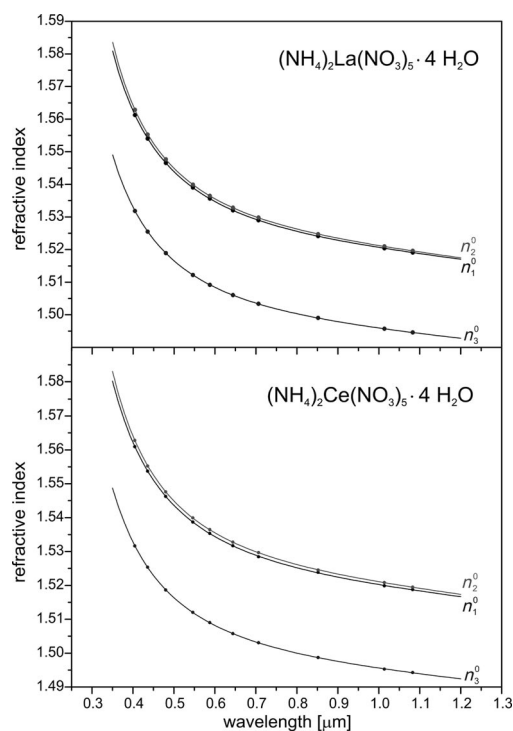


Figure 3. Principal refractive indices and their dispersion of crystals of $(\text{NH}_4)_2\text{La}(\text{NO}_3)_5 \cdot 4\text{H}_2\text{O}$ (top) and of $(\text{NH}_4)_2\text{Ce}(\text{NO}_3)_5 \cdot 4\text{H}_2\text{O}$ (bottom). Symbols indicate experimental refractive index data, lines indicate the fitted Sellmeier functions.

Table 2. Sellmeier coefficients for crystals of $(\text{NH}_4)_2\text{La}(\text{NO}_3)_5 \cdot 4\text{H}_2\text{O}$ and $(\text{NH}_4)_2\text{Ce}(\text{NO}_3)_5 \cdot 4\text{H}_2\text{O}$; the wavelength in the Sellmeier equation is in μm (ξ^2 is the sum of the residuals of the fit).

	D_1	D_2	D_3	D_4	ξ^2
$(\text{NH}_4)_2\text{La}(\text{NO}_3)_5 \cdot 4\text{H}_2\text{O}$					
n_1^0	2.3067(1)	0.01734(5)	0.0331(3)	0.0122(1)	8.1×10^{-11}
n_2^0	2.3097(7)	0.0172(2)	0.037(1)	0.0133(5)	1.9×10^{-9}
n_3^0	2.2324(1)	0.01532(4)	0.0316(2)	0.01029(8)	4.6×10^{-11}
$(\text{NH}_4)_2\text{Ce}(\text{NO}_3)_5 \cdot 4\text{H}_2\text{O}$					
n_1^0	2.305(2)	0.0178(6)	0.031(3)	0.012(1)	1.3×10^{-8}
n_2^0	2.308(1)	0.0177(3)	0.034(2)	0.0127(7)	3.9×10^{-9}
n_3^0	2.2313(9)	0.0155(3)	0.030(2)	0.0104(6)	2.9×10^{-9}

Sellmeier coefficients are given in Table 2. Crystals of $(\text{NH}_4)_2\text{La}(\text{NO}_3)_5 \cdot 4\text{H}_2\text{O}$ and $(\text{NH}_4)_2\text{Ce}(\text{NO}_3)_5 \cdot 4\text{H}_2\text{O}$ are biaxial negative; however, the birefringence $\Delta n = n_2^0 - n_1^0$ is very small. The angle $2V_a$ between the optic axes (Figure 4) ranges, for wavelengths between 0.365 and 1.083 μm , from 30° to 16° and from 31° to 20° for the La and the Ce compound, respectively. In monoclinic crystals, the orientation of the principal axes of the optical indicatrix, denoted by $\{\vec{e}_i^0\}$ in this work, that is, the orientation of the directions where the principal refractive indices of the crystals are found, is fixed only for \vec{e}_2^0 with $\vec{e}_2^0 \parallel \vec{a}_2 \parallel \vec{z}$, while the orientation of \vec{e}_1^0 and \vec{e}_3^0 generally varies within the plane (010) with the wavelength of light.

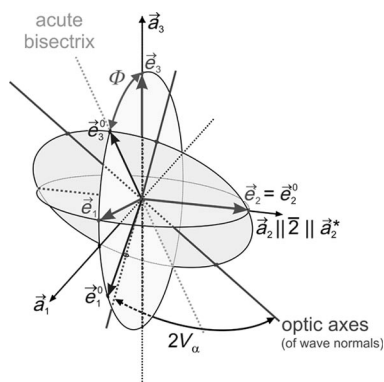


Figure 4. Mutual orientation of the crystallographic reference system $\{\vec{a}_i\}$, the crystal physical Cartesian system $\{\vec{e}_i^0\}$ and the system of principal axes of the optical indicatrix $\{\vec{e}_i^0\}$ for crystals of $(\text{NH}_4)_2\text{La}(\text{NO}_3)_5 \cdot 4\text{H}_2\text{O}$ and $(\text{NH}_4)_2\text{Ce}(\text{NO}_3)_5 \cdot 4\text{H}_2\text{O}$.

This wavelength-dependent rotational degree of freedom of the principal axes \vec{e}_1^0 and \vec{e}_3^0 around the \vec{z} axis, known as dispersion of the vibration directions, can be observed with white light on (010) plates of the title crystals as bluish or reddish colours when the crystals are slightly rotated off the position of maximum extinction in both directions between crossed polarizers. In Figure 4, where the mutual orientation of the crystallographic reference system $\{\vec{a}_i\}$, the crystal physical Cartesian system $\{\vec{e}_i^0\}$ and the system of principal axes of the optical indicatrix $\{\vec{e}_i^0\}$ is sketched for the investigated crystals, this orientation angle is denoted by Φ (i.e. the extinction angle of the crystal with respect to the \vec{a}_3 axis for a light wave propagation along \vec{e}_2). Values of Φ calculated for $(\text{NH}_4)_2\text{La}(\text{NO}_3)_5 \cdot 4\text{H}_2\text{O}$ and $(\text{NH}_4)_2\text{Ce}(\text{NO}_3)_5 \cdot 4\text{H}_2\text{O}$ from the refractive index data (and by

using the monoclinic angle a_2 given in Table 3) are given in Figure 5. They are in good agreement with the values measured for $\lambda = 0.5467 \mu\text{m}$.

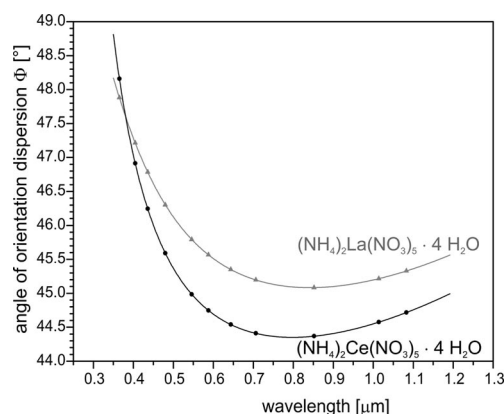


Figure 5. Wavelength dispersion of the orientation angle $\Phi = \angle(\vec{e}_3^0, \vec{a}_3)$ for crystals of $(\text{NH}_4)_2\text{La}(\text{NO}_3)_5 \cdot 4\text{H}_2\text{O}$ and $(\text{NH}_4)_2\text{Ce}(\text{NO}_3)_5 \cdot 4\text{H}_2\text{O}$. Symbols: calculated from measured refractive index data; lines: calculated from Sellmeier coefficients.

The precision refractive indices (with errors less than 1×10^{-4}) and their dispersion allow an analysis of conditions for phase matching of different nonlinear optical frequency conversion processes. In the present work, we focus in particular on the conditions for collinear second harmonic generation (SHG). In both crystals, $(\text{NH}_4)_2\text{La}(\text{NO}_3)_5 \cdot 4\text{H}_2\text{O}$ and $(\text{NH}_4)_2\text{Ce}(\text{NO}_3)_5 \cdot 4\text{H}_2\text{O}$, collinearly phase-matched SHG processes of type I phase matching (with ss-f interaction; s = slow wave, f = fast wave) can be realized, while type II phase matching (with sf-f interaction) is not possible. Phase-matching loci for several wavelengths of the fundamental wave are presented as Hobden plots [i.e. stereographic projections using the reference system $\{\vec{e}_i^0\}$]^[30] for both crystals in Figure 6. Noncritical phase matching type I is possible at a wavelength λ_f of the fundamental wave with wave normal \vec{k} parallel to \vec{e}_1^0 of $\lambda_f = 0.893 \mu\text{m}$ for $(\text{NH}_4)_2\text{La}(\text{NO}_3)_5 \cdot 4\text{H}_2\text{O}$ and of $\lambda_f = 0.892 \mu\text{m}$ for $(\text{NH}_4)_2\text{Ce}(\text{NO}_3)_5 \cdot 4\text{H}_2\text{O}$. For \vec{k} parallel to \vec{e}_2^0 , noncritical phase matching type I can be realized at $\lambda_f = 0.905 \mu\text{m}$ and at $\lambda_f = 0.909 \mu\text{m}$ for the La and the Ce compound, respectively. Note that the point group symmetry m of the crystals allows nonzero effective coefficients $d_{\text{eff}}^{\text{SHG}}$ of the SHG tensor for both directions of noncritical phase matching type I in the crystals, for example, d_{311}^{SHG} for incidence along \vec{e}_2^0 and

d_{322}^{SHG} for incidence along \vec{e}_1^0 . The results indicate that the SHG phase-matching properties of crystals of $(\text{NH}_4)_2\text{Ln}(\text{NO}_3)_5 \cdot 4\text{H}_2\text{O}$ ($\text{Ln} = \text{La}, \text{Ce}$) are rather insensitive to the kind of rare earth constituent. This continues a trend that could be observed already from the comparison of rubidium rare earth nitrate tetrahydrates $\text{Rb}_2\text{Ln}(\text{NO}_3)_5 \cdot 4\text{H}_2\text{O}$ ($\text{Ln} = \text{La}, \text{Ce}$) and the potassium compounds, $\text{K}_2\text{Ln}(\text{NO}_3)_5 \cdot 2\text{H}_2\text{O}$ ($\text{Ln} = \text{La}, \text{Ce}$), where the latter, however, possess a related but different crystal structure with orthorhombic symmetry $Fdd2$. Irrespective of this difference, the sensitivity of SHG phase-matching behaviour on the rare earth constituent decreases markedly within the series potassium \rightarrow rubidium \rightarrow ammonium rare earth nitrate hydrates: For $\text{K}_2\text{Ln}(\text{NO}_3)_5 \cdot 2\text{H}_2\text{O}$ ($\text{Ln} = \text{La}, \text{Ce}$), a fine-tuning of noncritical SHG phase matching (type I) is possible within a range from 1.055 to 1.107 μm by synthesis of mixed crystals;^[19] for $\text{Rb}_2\text{Ln}(\text{NO}_3)_5 \cdot 4\text{H}_2\text{O}$ ($\text{Ln} = \text{La}, \text{Ce}$), this range is reduced to 26 nm in the region between 0.876 and 0.902 μm ,^[11] while for $(\text{NH}_4)_2\text{Ln}(\text{NO}_3)_5 \cdot 4\text{H}_2\text{O}$ ($\text{Ln} = \text{La}, \text{Ce}$) noncritical SHG phase-matching conditions are virtually identical.

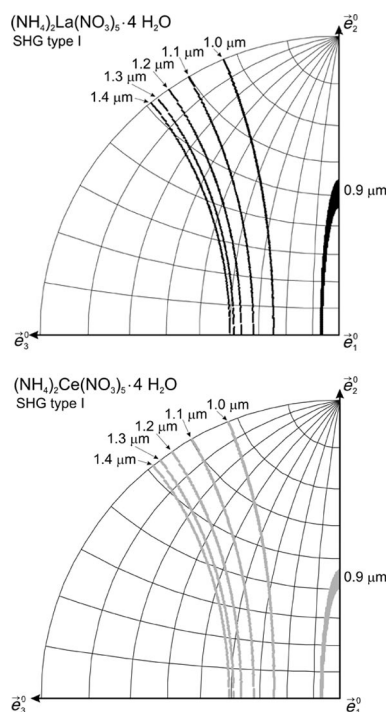


Figure 6. Stereographic projections of phase-matching (type I) loci for collinear second harmonic generation (Hobden plots) for different fundamental wavelengths in $(\text{NH}_4)_2\text{La}(\text{NO}_3)_5 \cdot 4\text{H}_2\text{O}$ (top) and $(\text{NH}_4)_2\text{Ce}(\text{NO}_3)_5 \cdot 4\text{H}_2\text{O}$ (bottom).

Conclusions

The results of this work prove that the ammonium rare earth nitrate tetrahydrates $(\text{NH}_4)_2\text{Ln}(\text{NO}_3)_5 \cdot 4\text{H}_2\text{O}$ form an isomorphic series of non-centrosymmetric polar crystals for $\text{Ln} = \text{La}, \text{Ce}, \text{Pr}, \text{Nd}$ and are further isomorphic to the corresponding rubidium compounds $\text{Rb}_2\text{Ln}(\text{NO}_3)_5 \cdot 4\text{H}_2\text{O}$.

As shown for the examples of the lanthanum and the cerium compounds, crystals of $(\text{NH}_4)_2\text{Ln}(\text{NO}_3)_5 \cdot 4\text{H}_2\text{O}$ can be grown to large single crystals of optical quality. The refractive indices and their dispersion, determined for the La and Ce compounds, allow the realization of phase-matching conditions for second harmonic generation. With these properties the crystals meet the basic requirements for being worthwhile for further investigations of their nonlinear optical properties.

Experimental Section

Crystal Structure Determination

The longitudinal piezoelectric effect was detected for large single crystals of the La and Ce compounds with a charge amplifier (Kistler, Type 5011) and an analogue peak indicator (Kistler, Type 5511) by application of uniaxial stress to crystal faces $\{100\}$ and $\{001\}$. The setup was also used for the detection of charge of pyroelectric origin arising by change of temperature.

For crystal structure determination, a data set for each of the four compounds $(\text{NH}_4)_2\text{Ln}(\text{NO}_3)_5 \cdot 4\text{H}_2\text{O}$ ($\text{Ln} = \text{La}, \text{Ce}, \text{Pr}, \text{Nd}$) was collected at 298 K with a Nonius Kappa CCD diffractometer, equipped with a rotating anode generator (Mo- K_α radiation, $\lambda = 0.71073 \text{ \AA}$) and focusing mirror. Data collection was performed with the Nonius COLLECT (Nonius B.V., 1998) software package, data reduction by using Denzo-SMN^[31] and absorption correction with Denzo.^[32] The structures were solved by direct methods with SHELXS-97^[33] and refined by the full-matrix least-squares method based on F^2 (SHELXL-97)^[34] with anisotropic thermal parameters for all non-hydrogen atoms. For the calculations, the distances N–H and O–H were fixed to 0.95(2) \AA . The graphics were produced with ATOMS.^[35] Crystal data and details of data collection and structure refinement are given in Table 3.

Further details on the crystal structure investigations may be obtained from the Fachinformationszentrum Karlsruhe, 76344 Eggenstein-Leopoldshafen, Germany (fax: +49-7247-808-666; e-mail: crysdata@fiz-karlsruhe.de), on quoting the depository numbers CSD-421602 for $(\text{NH}_4)_2\text{La}(\text{NO}_3)_5 \cdot 4\text{H}_2\text{O}$, -421601 for $(\text{NH}_4)_2\text{Ce}(\text{NO}_3)_5 \cdot 4\text{H}_2\text{O}$, -421604 for $(\text{NH}_4)_2\text{Pr}(\text{NO}_3)_5 \cdot 4\text{H}_2\text{O}$ and -421603 for $(\text{NH}_4)_2\text{Nd}(\text{NO}_3)_5 \cdot 4\text{H}_2\text{O}$.

Crystal Growth: Large single crystals of $(\text{NH}_4)_2\text{La}(\text{NO}_3)_5 \cdot 4\text{H}_2\text{O}$ and $(\text{NH}_4)_2\text{Ce}(\text{NO}_3)_5 \cdot 4\text{H}_2\text{O}$ were grown from acidic aqueous solutions (surplus of 3–5% HNO_3) containing a stoichiometric ratio of the constituents $[2\text{NH}_4\text{NO}_3 + 1\text{La}(\text{NO}_3)_3 \text{ or } 1\text{Ce}(\text{NO}_3)_3]$. Lanthanum nitrate was synthesized by dissolving La_2O_3 (Chempur, 99.99%) in nitric acid, cerium nitrate was purchased as the hexahydrate, $\text{Ce}(\text{NO}_3)_3 \cdot 6\text{H}_2\text{O}$ (Chempur, 99.9%), and commercially available ammonium nitrate (Merck, 99.0%) was used. The growth process was performed for both compounds in 3 L crystallization vessels, held at constant temperature of 38 $^\circ\text{C}$, by slow controlled evaporation of the solvent. The evaporation rate was adjusted to achieve a linear growth rate of approximately 0.3 mm/day for the La compound and of ca. 0.2 mm/day for the Ce compound. Seed crystals were suspended on platinum wire. In our experiments, a growth period of 12–16 weeks was typically applied. Small crystals of $(\text{NH}_4)_2\text{Nd}(\text{NO}_3)_5 \cdot 4\text{H}_2\text{O}$ and $(\text{NH}_4)_2\text{Pr}(\text{NO}_3)_5 \cdot 4\text{H}_2\text{O}$ for X-ray structure determination were synthesized at 20 $^\circ\text{C}$ from aqueous solutions of the nitrates NH_4NO_3 and $\text{Ln}(\text{NO}_3)_3$ ($\text{Ln} = \text{Nd}, \text{Pr}$) in the stoichiometric ratio $2\text{NH}_4:1\text{Ln}$ with ca. 5% HNO_3 added. The solutions of the rare earth nitrates were prepared by dissolving of

Table 3. Crystal data, structure determination and refinement summary for (NH₄)₂La(NO₃)₅·4H₂O (1), (NH₄)₂Ce(NO₃)₅·4H₂O (2), (NH₄)₂Pr(NO₃)₅·4H₂O (3) and (NH₄)₂Nd(NO₃)₅·4H₂O (4). All data were collected at 298 K.

	1	2	3	4
Empirical formula	H ₁₆ LaN ₇ O ₁₉	H ₁₆ CeN ₇ O ₁₉	H ₁₆ N ₇ PrO ₁₉	H ₁₆ N ₇ NdO ₁₉
Formula mass	557.11	558.32	559.11	562.44
Crystal system	monoclinic	monoclinic	monoclinic	monoclinic
Space group	Cc	Cc	Cc	Cc
<i>a</i> (= <i>a</i> ₁) [Å]	11.1347(2)	11.0786(4)	11.0677(5)	11.0430(4)
<i>b</i> (= <i>a</i> ₂) [Å]	8.9389(1)	8.9289(3)	8.9184(2)	8.9113(3)
<i>c</i> (= <i>a</i> ₃) [Å]	17.9450(3)	17.9042(9)	17.9195(7)	17.9011(4)
β (= α_2) [°]	101.797(1)	101.782(2)	101.883(2)	101.821(1)
<i>V</i> [Å ³]	1748.38(5)	1733.76(12)	1730.86(11)	1724.24(9)
$\rho_{\text{calcd.}}$ [g cm ⁻³]	2.116	2.139	2.146	2.167
<i>Z</i>	4	4	4	4
<i>F</i> (000)	1096	1100	1104	1108
μ [mm ⁻¹]	2.554	2.737	2.927	3.124
Crystal size [mm]	0.30 × 0.28 × 0.25	0.30 × 0.15 × 0.05	0.30 × 0.25 × 0.15	0.35 × 0.35 × 0.15
2 θ range [°]	4.56 to 30.0	4.27 to 30.0	4.27 to 30.0	3.04 to 29.99
Limiting indices	−15 ≤ <i>h</i> ≤ 15 −12 ≤ <i>k</i> ≤ 11 −25 ≤ <i>l</i> ≤ 25	−15 ≤ <i>h</i> ≤ 15 −12 ≤ <i>k</i> ≤ 11 −25 ≤ <i>l</i> ≤ 25	−15 ≤ <i>h</i> ≤ 15 −6 ≤ <i>k</i> ≤ 12 −25 ≤ <i>l</i> ≤ 25	−15 ≤ <i>h</i> ≤ 15 −12 ≤ <i>k</i> ≤ 10 −25 ≤ <i>l</i> ≤ 25
Reflections collected/ unique with <i>I</i> > 2 σ (<i>I</i>)	6809/4121	8430/4238	7085/3130	8109/4306
Parameters	280	292	292	280
GoF on <i>F</i> ²	1.040	1.035	1.064	1.086
<i>R</i> [<i>I</i> > 2 σ (<i>I</i>)]	0.0314	0.0395	0.0325	0.0385
<i>R</i> _w	0.0821	0.1054	0.0847	0.0990
($\Delta\rho$) _{max} /($\Delta\rho$) _{min} [e·Å ⁻³]	2.032/−0.958	1.825/−1.427	1.172/−2.210	1.666/−3.008

Nd₂O₃ (Alfa, 99.9%) and Pr₆O₁₁ (Alfa Aesar, 99.9%), respectively, in nitric acid with a small surplus of HNO₃. Both compounds are sensitive to humidity.

Optical Properties: Crystals of monoclinic symmetry, such as the title compounds, possess three principal refractive indices n_1^0 , n_2^0 , n_3^0 . They were determined for crystals of the colourless compounds (NH₄)₂La(NO₃)₅·4H₂O and (NH₄)₂Ce(NO₃)₅·4H₂O by the prism method and normal incidence by using two prisms with incidence face (010) (prism I) and (001) (prism II), respectively, for each compound. Measurements with prisms I yield n_1^0 and n_3^0 , measurements with prism II yield n_2^0 and n' , with

$$n' = \frac{(n_1^0 \cdot n_3^0)^2}{\sqrt{[(n_1^0 \cdot \sin \eta)^2 + (n_3^0 \cdot \cos \eta)^2]}}$$

[η = wavelength-dependent angle between face normal $\vec{h}^*(001)$ and the relevant principal axis of the optical indicatrix, here \vec{e}_3^0].

For both compounds, data were collected at 11 discrete wavelengths in the region between 0.365 μm and 1.083 μm with a goniometer-spectrometer system (Möller-Wedel; for instrumental details see^[36,37]). The measured data were corrected for the refractive index of air and its dispersion by $n^{\text{corr.}} = n^{\text{meas.}} \times n^{\text{air}}$, with data from ref.^[38] The extinction angle with respect to the edge between the faces (010) and (001), which has the direction of \vec{a}_1 , was measured on a plate (010) with a polarizing microscope, by using an interference green filter with ca. 70% transmission at 0.5467 μm .

Acknowledgments

We thank our technical staff members Steffi Seidel and Nina Gelewski, Institute of Crystallography, University of Cologne, for technical assistance with crystal growth.

- [1] C. Auer v. Welsbach, *Monatsh. Chem.* **1885**, 6, 477–491.
- [2] M. C. Marignac, *Ann. Chim. Phys. (Sér. 4)* **1873**, 30, 45–69.
- [3] M. Descloizeaux, *Ann. Mines* **1858**, 14, 339–420.
- [4] M. H. Dufet, *Bull. Soc. Fr. Mineral. Crystallogr.* **1888**, 11, 143–148.
- [5] A. Fock, *Z. Kristallogr.* **1894**, 22, 29–42.
- [6] E. H. Kraus, *Z. Kristallogr.* **1901**, 34, 397–431.
- [7] M. G. Wyruboff, *Bull. Soc. Fr. Mineral. Crystallogr.* **1907**, 30, 299–323.
- [8] G. Jantsch, S. Wigdorow, *Z. Anorg. Allg. Chem.* **1911**, 69, 221–231.
- [9] A. G. Vigdorich, Y. A. Malinovskii, A. G. Dryuchko, V. B. Kalinin, I. A. Verin, S. Y. Stefanovich, *Sov. Phys. Crystallogr.* **1992**, 37, 783–791.
- [10] N. Audebrand, J. P. Auffrédic, M. Louër, N. Guillou, D. Louër, *Solid State Ionics* **1996**, 84, 323–333.
- [11] L. Bohatý, P. Held, P. Becker, *Z. Anorg. Allg. Chem.* **2009**, 635, 2236–2241.
- [12] B. Eriksson, L. O. Larsson, L. Niinistö, *Acta Chem. Scand., Ser. A* **1982**, 36, 465–470.
- [13] G. Meyer, E. Manek, A. Reller, *Z. Anorg. Allg. Chem.* **1990**, 591, 77–86.
- [14] M. Najafpour, P. Starynowicz, *Acta Crystallogr., Sect. E* **2006**, 62, i145–i146.
- [15] B. Eriksson, L. O. Larsson, L. Niinistö, J. Valkonen, *Acta Chem. Scand., Ser. A* **1980**, 34, 567–572.
- [16] P. Held, H. Hellwig, S. Rühle, L. Bohatý, *J. Appl. Crystallogr.* **2000**, 33, 372–379.
- [17] C. A. Ebberts, L. D. DeLoach, M. Webb, D. Eimerl, S. P. Velsko, D. A. Keszler, *IEEE J. Quantum Electron.* **1993**, 29, 497–507.
- [18] H. Hellwig, S. Rühle, P. Held, L. Bohatý, *J. Appl. Crystallogr.* **2000**, 33, 380–386.
- [19] L. Bohatý, P. Becker, *Cryst. Res. Technol.* **2009**, 44, 1131–1138.
- [20] N. Audebrand, D. Louër, *Acta Crystallogr., Sect. C* **2000**, 56, 913–915.

- [21] S. Stockhausen, G. Meyer, *Z. Kristallogr. - New Cryst. Struct.* **1997**, *212*, 317–318.
- [22] A. G. Vigdorchik, Y. A. Malinovskii, V. I. Adrianov, A. G. Dryuchko, *Izv. Akad. Nauk SSSR, Neorg. Mater.* **1990**, *26*, 2357–2362.
- [23] N. Audebrand, J. P. Auffrédic, D. Louër, *J. Solid State Chem.* **1997**, *132*, 361–371.
- [24] W. T. Dong, H. J. Zhang, Q. Su, Y. H. Lin, S. M. Wang, C. S. Zhu, *J. Solid State Chem.* **1999**, *148*, 302–307.
- [25] A. G. Vigdorchik, Y. A. Malinovskii, A. G. Dryuchko, I. A. Verin, *Sov. Phys. Crystallogr.* **1992**, *37*, 466–469.
- [26] A. G. Vigdorchik, Y. A. Malinovskii, A. G. Dryuchko, *Sov. Phys. Crystallogr.* **1990**, *35*, 823–825.
- [27] A. G. Vigdorchik, Y. A. Malinovskii, A. G. Dryuchko, *Sov. Phys. Crystallogr.* **1990**, *35*, 826–828.
- [28] A. G. Vigdorchik, Y. A. Malinovskii, A. G. Dryuchko, *Sov. Phys. Crystallogr.* **1989**, *34*, 170–173.
- [29] P. H. Egli, *Am. Mineral.* **1948**, *33*, 622–633.
- [30] M. V. Hobden, *J. Appl. Phys.* **1967**, *38*, 4365–4372.
- [31] Z. Otwinowski, W. Minor, *Methods Enzymol.* **1997**, *276*, 307–326.
- [32] Z. Otwinowski, D. Borek, W. Majewski, W. Minor, *Acta Crystallogr., Sect. A* **2003**, *59*, 228–234.
- [33] G. M. Sheldrick, *Acta Crystallogr., Sect. A* **1990**, *46*, 467–473.
- [34] G. M. Sheldrick, *Acta Crystallogr., Sect. A* **2008**, *64*, 112–122.
- [35] E. Dowty, *ATOMS Version 6.0, Shape Software*, **2002**.
- [36] L. Bohatý, H. Hellwig, S. Ahrweiler, A. Möller, *Cryst. Res. Technol.* **1999**, *34*, 533–537.
- [37] P. Becker, P. Held, J. Liebertz, L. Bohatý, *Cryst. Res. Technol.* **2009**, *44*, 603–612.
- [38] K. P. Birch, M. J. Downs, *Metrologia* **1994**, *31*, 315–316.

Received: February 14, 2010

Published Online: May 27, 2010